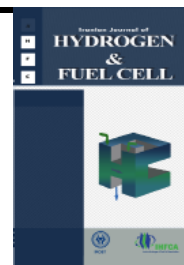


Iranian Journal of Hydrogen & Fuel Cell

IJHFC

Journal homepage://ijhfc.irostd.ir



A high performance lithium-ion battery using $\text{LiNa}_{0.02}\text{K}_{0.01}\text{FePO}_4/\text{C}$ as cathode material and anatase TiO_2 nanotube arrays as anode material

Reza Daneshtalab¹, Ali Reza Madram^{1,*}, Mohammad Reza Sovizi¹

¹Faculty of Chemistry and Chemical Engineering, Malek-Ashtar University of Technology, Tehran, IRAN

Article Information

Article History:

Received:

24 June 2017

Received in revised form:

18 July 2017

Accepted:

06 Aug 2017

Keywords

Lithium-ion battery (LIB)

Lithium iron phosphate

TiO_2 nanotube arrays (TNAs)

Full-cell

Electric vehicles (EVs)

Abstract

In this paper we report on a lithium ion battery (LIB) based on improved olivine lithium-iron phosphate/carbon (LiFePO_4/C) as cathode material and $\text{LiNa}_{0.02}\text{K}_{0.01}\text{FePO}_4/\text{C}$ synthesized by sol-gel method as cathode material and TiO_2 nanotube arrays (TNAs) with an anatase phasesynthesized through anodization of Ti foil as an anode electrode. Crystallographic structure and surface morphology of the cathode and anode materials were studied using X-ray diffraction (XRD) and scanning electron microscopy (SEM). The electrochemical characterization of the $\text{Li-LiNa}_{0.02}\text{K}_{0.01}\text{FePO}_4/\text{C}$ and Li-TNAs half-cells and $\text{LiNa}_{0.02}\text{K}_{0.01}\text{FePO}_4/\text{C-TNAs}$ full-cell configuration was carried out through cyclic voltammetry (CV) and charge/discharge analysis. The operating potential and the first discharge capacity of the full cell were about 1.7 V and 127 mAhg^{-1} (at 0.5 C), respectively, and stayed stable for up to 100 cycles with limited capacity fading. Therefore, this system (full-cell) is characterized by enhanced electrochemical properties, a high safety level, remarkable environmental compatibility, long life and low cost. The preliminary results in this work suggest that the system may be suitable for using as environmental friendly hybrid, electric vehicles (EVs), and an alternative energy storage system for powering safe and stationary applications.

1. Introduction

Lithium ion batteries (LIBs) are reported as very appealing energy storage systems characterized

by very high energy density and power density compared to conventional batteries. Electric vehicles (EVs) and hybrid electric vehicles (HEVs) systems require batteries with high power density

*Corresponding Author's Fax: +98-21-22962257

E-mail address: armadram@mut.ac.ir

and excellent cycling stability. In addition, special attention should be paid to the safety of EVs and HEVs [1]. In order to achieve this matter, we should seek to promote the best cell configuration through modification of electrode materials. The present configuration of LIBs contains a lithium cobalt oxide cathode and a graphite anode. Cobalt is an expensive and toxic metal. Also, graphite is characterized by a very low working voltage, i.e. 0.1-0.2 V relative to lithium, which is outside the electrochemical stability windows of the organic electrolytes [2]. In recent years new materials, such as layered structures, olivine and spinel structures, have been used as cathode material; and $\text{Li}_4\text{Ti}_5\text{O}_{12}$ (LTO) [3, 4], Li-alloying (Sn-C) [5, 6], and TiO_2 nanoparticles have been used as anode material in the literature [2]. Among the cathode materials lithium iron phosphate, which is a P-type semiconductor containing a stable working voltage of 3.5 V vs. Li and specific capacity of 170 mAhg^{-1} [2], is a much more popular cathode material in LIBs than other cathode materials due to its high environmental compatibility, low cost, improved safety and flat charge/discharge curves during the two-phase Li-insertion/extraction process, and excellent cycling stability [7, 8]. Titania, (TiO_2), as an n-type semiconductor contains different types of crystalline structures such as rutile, anatase, brookite, etc. It has great prospects for use as an anode material for LIBs due to its non-toxicity, low-cost, safer insertion/extraction potential toward lithium (Li), relatively high Li storage capacity, excellent structural stability, good rate property and lack of decomposition of organic electrolyte and electrochemical Li deposition, which is necessary for the safety of power type LIBs [9]. In addition, TiO_2 anodes have some advantages over conventional carbon or metal-oxide anodes such as avoiding the formation of lithium dendrites [10], high thermal stability, low volume change during cycling and a high operating rate [11]. Among the crystalline structures of TiO_2 , the anatase structure shows promising characteristics, such as less volume change during Li-ion insertion/extraction (about 3.7%) and the highest theoretical capacity, and

thus is a forthcoming electrode material for LIBs [12, 13]. It is worth mentioning that the Li storage capability of TiO_2 strongly depends on its structural parameters such as crystallinity, phase structure, morphology, particle size, and pore characteristics [9]. Unfortunately, TiO_2 has poor electronic and ionic conductivity. In order to improve the poor electronic and ionic conductivity of TiO_2 , nano- TiO_2 structures with various morphologies, such as nanotubes, have been synthesized [14]. The synthesized anatase TiO_2 nanotubes demonstrated excellent electrochemical properties with respect to TiO_2 nanoparticles and were very promising for electrodes in LIB applications, as reported in the literature [12]. Also, nanotubular structure leads to a large specific surface area increasing the contact area with liquid electrolyte, shortening transportation distances for both Li ions and electrons, improving the kinetics of Li intercalation, and de-intercalating at the electrode-electrolyte interface which accelerates Li ion diffusion and improves the cycle stability [14]. Therefore, TiO_2 nanotube structures are very promising for application in Li-ion batteries with high-rate charge/discharge properties [15] and for the fabrication of nanostructured thin-film microbatteries [16]. Several studies have been reported on TiO_2 properties as anode material in the half cell of the LIBs [10, 16-19]. In addition, there are a few reports on the electrochemical properties of the full cell of Li-ion batteries using LiMn_2O_4 [20-22] or LiFePO_4 [2, 7, 13, 23, 24] as cathode material and TiO_2 as anode material. Nevertheless, systems achieved by coupling titanium dioxide anodes with low-voltage cathode materials, such as LiFePO_4 which work at lower voltage, have been suggested. This system can be suitable for stationary applications where the energy density of the system has a secondary importance with respect to other parameters such as power and system cost [24]. To the best of our knowledge, there is no report in the literature indicating the use of improved LiFePO_4 composition and TiO_2 nanotube arrays (TNAs) as cathode and anode materials, respectively, in a full cell configuration. In this study, we focus on the

use of $\text{LiNa}_{0.02}\text{K}_{0.01}\text{FePO}_4/\text{C}$ as cathode material [25] and TNAs as anode material in LIBs [26]. Then, the electrochemical properties of the half cell and full cell configurations of the Li-ion battery are considered and compared with each other. Our results showed that the electrochemical performance of TNAs as anode material in a full cell configuration is better than electrospun TiO_2 nanofibers [13] and TiO_2 nanoparticles powder [7].

2. Experimental

2.1. Material preparation

LiFePO_4/C as cathode material was synthesized by the sol-gel method in our previous work and improved by doping of Na and K ions to produce a $\text{LiNa}_{0.02}\text{K}_{0.01}\text{FePO}_4/\text{C}$ structure [25]. Briefly, the $\text{LiNa}_{0.02}\text{K}_{0.01}\text{FePO}_4/\text{C}$ composites were prepared from lithium hydroxide monohydrate $\text{LiOH}\cdot\text{H}_2\text{O}$ ($\geq 99.0\%$ Fluka), ferric nitrate $\text{Fe}(\text{NO}_3)_3\cdot 9\text{H}_2\text{O}$ (A.C.S. Reagent), phosphoric acid H_3PO_4 (A.C.S. Reagent, min. 85%, Spectrum) as raw materials and $\text{NaNO}_3\cdot\text{H}_2\text{O}$ (99%, Aldrich) and $\text{KNO}_3\cdot\text{H}_2\text{O}$ (99%, Aldrich) as dopant materials. These materials were mixed in an atomic ratio of $(\text{Li}+\text{Na}+\text{K}):\text{Fe}:\text{PO}_4$ (1:1:1). Citric acid $\text{C}_6\text{H}_8\text{O}_7$ ($\geq 99.0\%$, Sigma) was added to the raw materials as carbon source material and complexing agents to form the gel medium. As in a typical synthesis, H_3PO_4 and $\text{Fe}(\text{NO}_3)_3\cdot 9\text{H}_2\text{O}$ were first mixed and dissolved in deionized water. Then, $\text{LiOH}\cdot\text{H}_2\text{O}$ and stoichiometric amount of dopants were dissolved in the above solution, followed by slowly adding $\text{C}_6\text{H}_8\text{O}_7$ under constant stirring at room temperature. The obtained mixture was stirred at 70°C for 1h until the solution turned into a dark brownish transparent sol. The mixture was dried in an oven at 120°C for 6 h, then heated at 350°C for 1 h in argon flow. Finally, the produced sample was sintered at 700°C for 15 h in an Ar + 5% H_2 atmosphere flow.

TNAs with anatase structure as the anode material have already been reported in a previous paper [26].

Briefly, TNAs were synthesized by the anodization method in a two-electrode cell configuration including Ti foil (99.7%) as working(working what?) and platinum foil as counter electrodes at applied constant voltage of 50 V for 4 h. The anodizing bath contained NH_4F (0.3% w/w) in a mixture of deionized water and ethylene glycol (2:98 w/w). Finally, the synthesized TNAs were washed with ethanol and deionized water several times and annealed at 450°C for 3 h with a temperature ramp rate of $1^\circ\text{C}/\text{min}$ under ambient air to obtain crystalline TNAs on the Ti foil.

2.2. Structural characterization

X-ray diffraction (XRD) patterns were obtained by (D5000, Siemens Co.) using graphite-monochromatized Cu $\text{K}\alpha$ radiation ($\lambda = 1.5418 \text{ \AA}$, 40 kV, 30 mA). The morphology of the products were studied by a scanning electron microscope (SEM, XL30 Philips Co.) equipped with an energy dispersive spectrometer (EDS).

2.3. Electrochemical measurements

The working electrode was prepared by mixing the produced powders ($\text{LiNa}_{0.02}\text{K}_{0.01}\text{FePO}_4/\text{C}$ composites) with acetylene black (Beijing Chemical Reagents Corporation, China) as a conductor, and polyvinylidene fluoride (PVDF, Shanghai Chemical Reagents Corporation, China) as a binder, in a weight ratio of 80:10:10 in N-methyl-2-pyrrolidone (NMP, Shanghai Chemical Reagents Corporation, China). The slurry was coated onto a non-corrosive stainless steel current collector at 20 MPa and dried at 120°C for 12 h in the vacuum oven [25]. The performance of $\text{LiNa}_{0.02}\text{K}_{0.01}\text{FePO}_4/\text{C}$ and TNAs electrodes were evaluated both in half (using a lithium foil as the counter electrode) and full cells (coin-type, size CR2032, Hohsen Corp., Japan) in 1 M LiPF_6 in EC:DMC:DEC (1:1:1) electrolyte solution with a polypropylene membrane separator (type 2400, Celgard, Inc., USA) assembled in an argon glove box (Mbraun, Unilab, Germany) at room temperature. The discharge tests were performed by galvanostatic

cycling in a potential range between 4.2 V and 2.5 V for Li-LiNa_{0.02}K_{0.01}FePO₄/C, between 2.7 V and 1 V for Li-TNAs half-cells and between 2.5 V and 1 V for LiNa_{0.02}K_{0.01}FePO₄/C-TNAs full-cell at various C rate currents at room temperature using a battery analyzer instrument. The CV tests for all cells were performed at a scan rate of 0.1 mVs⁻¹ and voltage ranges are as mentioned above. The electrochemical measurements were performed using a EG&G Potentiostat/Galvanostat, PARSTAT 2273. All potentials are cited with respect to the reference Li⁺/Li. It is worth noting that the maximum amount of x in Li_xTiO₂ was assumed to be 1 (corresponding to 335 mAh g⁻¹) and thus the charging rates in these measurements were based on a 1C rate of 0.335 A g⁻¹. For the LiNa_{0.02}K_{0.01}FePO₄/C electrode, the 1C rate was considered as 0.17 A g⁻¹. Also, the full cell in 1C rate of discharge state referred to the LiNa_{0.02}K_{0.01}FePO₄/C active mass as 0.17 A g⁻¹. It is worth mentioning that in half-cell configurations, metallic lithium acts as a reservoir for Li-ions, whereas in a full cell arrangement cathodes are the only source for Li-ions and it is highly limited. Thus, energy and power density were calculated based on the anode weight in the full cell, which is the limiting electrode. Hence, mass balance is necessary to satisfy the required amount of Li-ions during the charge-discharge process. Based on the full-cell configuration, mass balance between the electrodes is optimized for the ratio 2:1 (cathode with respect to anode) in such a way that the cathode and anode material loading were 4 and 2 mg/cm², respectively. Also, the loading of cathode and anode material in the half cell was 4 and 2 mg/cm², respectively.

3. Results and discussion

The structure and morphology of LiNa_{0.02}K_{0.01}FePO₄/C and TNAs electrodes were obtained by XRD and SEM techniques. Fig. 1 shows the XRD pattern, SEM image and EDS spectrums of LiNa_{0.02}K_{0.01}FePO₄/C nanocomposite that is characterized by a well-defined crystalline structure

and morphology. Also, Fig. 2 shows the XRD pattern, SEM image and EDS spectrums of TNAs grown on the Ti foil which reveals the formation of crystalline anatase TiO₂ nanotubes. Furthermore, it indicates that the inner diameter of the TNAs is about 110 nm. Fig. 3 shows the typical CV traces of Li-LiNa_{0.02}K_{0.01}FePO₄/C (between 2.5–4.2V), Li-TNAs (between 1–2.7V) in half-cells, and LiNa_{0.02}K_{0.01}FePO₄/C-TNAs (between 1–2.5V) in full-cell configurations, both recorded at a slow scan rate of 0.1 mV s⁻¹. The CV diagram of the full-cell showed the presence of sharp oxidation peaks at ~1.80 V (extraction of Li-ions from the cathode material and subsequent insertion of Li-ions into the anode material or in other words, oxidation of Fe²⁺ to Fe³⁺ and reduction of Ti⁴⁺ to Ti³⁺) and ~1.47 V (extraction of Li-ions from the anode material and simultaneous insertion of Li-ions into the cathode material or in other words, oxidation of Ti³⁺ to Ti⁴⁺ and reduction of Fe³⁺ to Fe²⁺) during the anodic and cathodic scans, respectively. This phenomenon indicates that the insertion and/or extraction of lithium ions occur in one stage. Also, the same area of the anodic and cathodic peak can be attributed to the excellent electrochemical cycling reversibility during electrochemical cycling according to the equilibrium, LiFePO₄ + TiO₂ ↔ FePO₄ + LiTiO₂. In recent studies, discharge potential curves for the first cycle and cycling performances of TNAs, LiNa_{0.02}K_{0.01}FePO₄/C composite and full-cell configuration are determined at various C rates from 0.1C to 5C, as shown in Fig. 4. As can be seen in Fig. 4a, the discharge curves have one voltage plateaus at around 1.7-1.8 V, which is associated with the result observed in the cyclic voltammogram. Also, the LiNa_{0.02}K_{0.01}FePO₄/C electrode is characterized by a flat potential at approximately 3.2-3.4 V vs. Li from two-phase Li-extraction /insertion in various C rates (Fig. 4b). Furthermore, the discharge curves of the LiNa_{0.02}K_{0.01}FePO₄/C-TNAs full-cell at various C rates shows a voltage plateaus at around 1.5-1.7 V (Fig. 4c). In a similar rate, the anatase TNAs also exhibited a much higher response rate than that of the LiNa_{0.02}K_{0.01}FePO₄/C electrode. As can be seen in

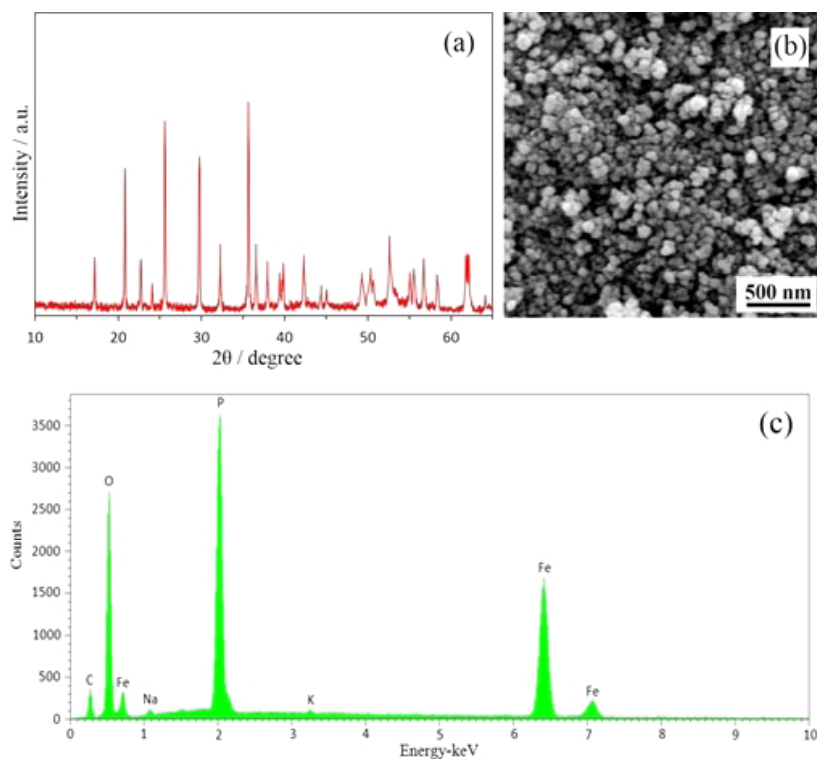


Fig. 1. a) XRD pattern, b) SEM image and c) EDS spectrum of $\text{LiNa}_{0.02}\text{K}_{0.01}\text{FePO}_4/\text{C}$ composite.

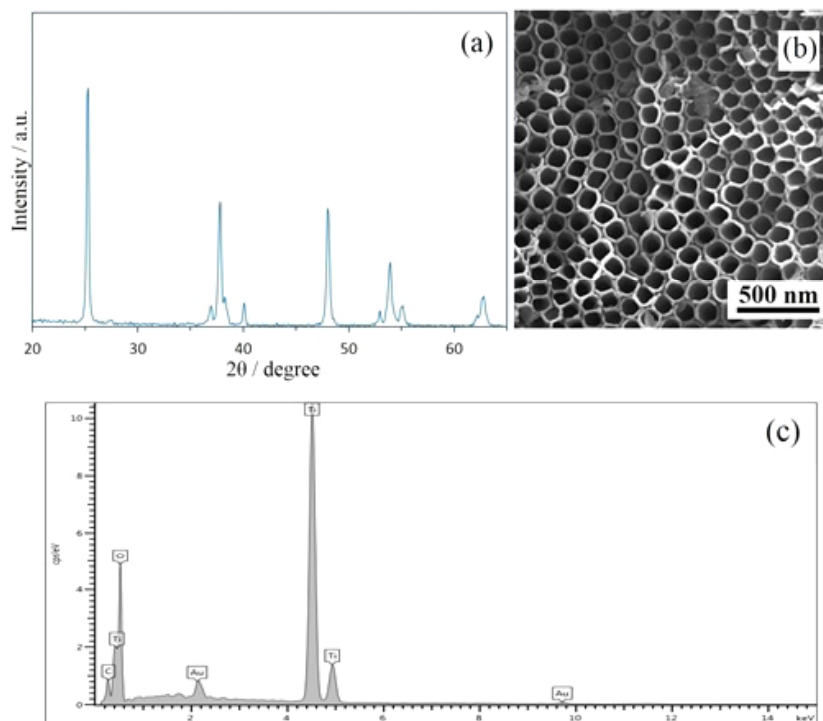


Fig. 2. a) XRD pattern, b) SEM image and c) EDS spectrum of TNAs.

Figure 4d, 4e and 4f, the first irreversible discharge capacity of the TNAs sample is higher than that of the $\text{LiNa}_{0.02}\text{K}_{0.01}\text{FePO}_4/\text{C}$ electrode and full cell

configuration. Shu et al. [27] reported that this phenomenon was mainly related to the electrolyte decomposition on the electrode surface, which is not

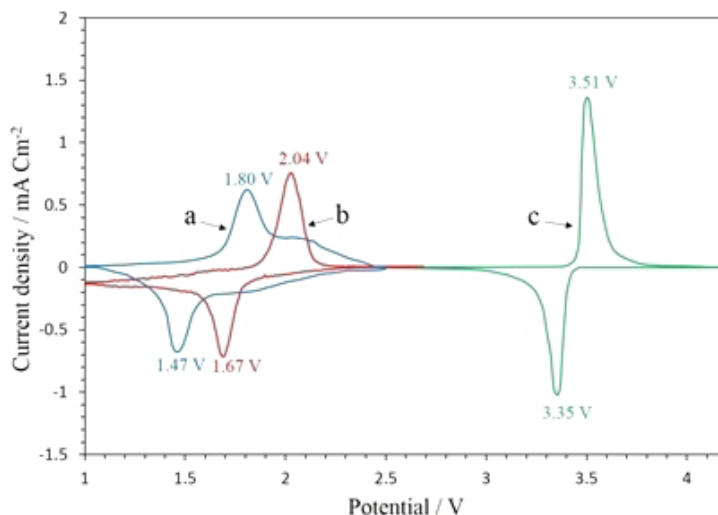


Fig. 3. Cyclic voltammogram (CV) of a) $\text{LiNa}_{0.02}\text{K}_{0.01}\text{FePO}_4/\text{C}$ -TNAs full-cell assembly cycled, b) and c) indicate the CV profiles of Li-TNAs and Li- $\text{LiNa}_{0.02}\text{K}_{0.01}\text{FePO}_4/\text{C}$ half-cells, respectively at a scan rate of 0.1 mV s^{-1} .

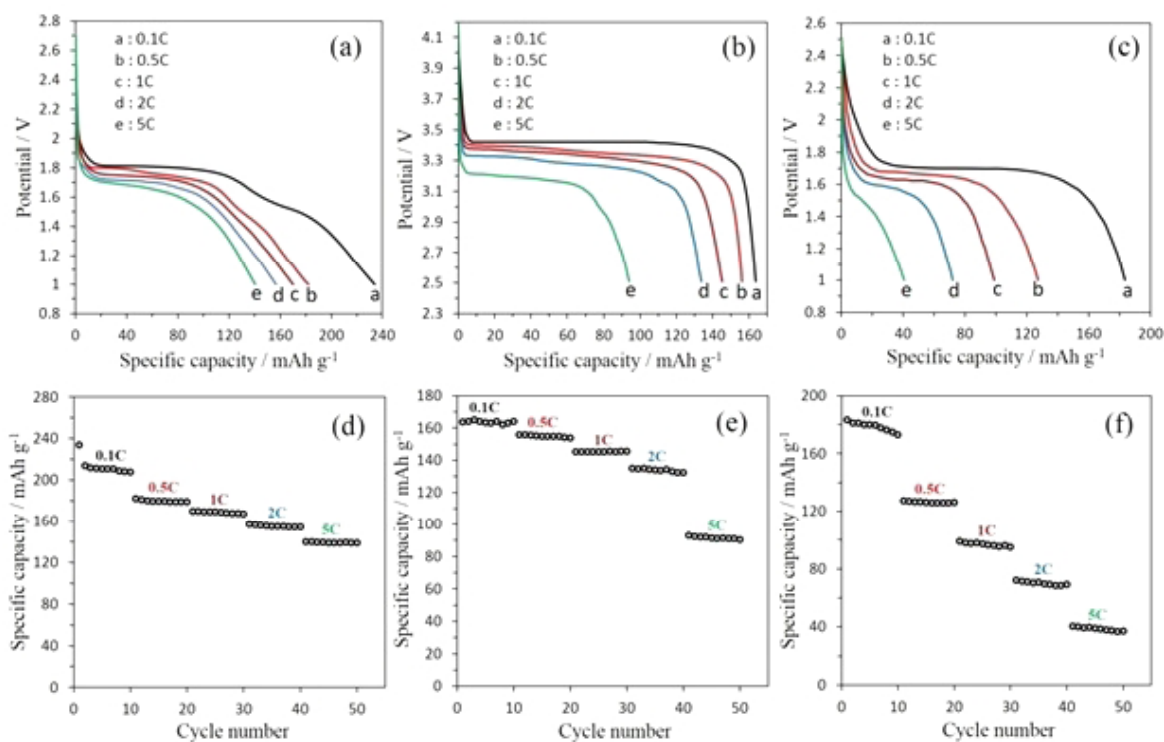


Fig. 4. voltage profiles of discharge at various C rates for a) TNAs, b) $\text{LiNa}_{0.02}\text{K}_{0.01}\text{FePO}_4/\text{C}$ and c) $\text{LiNa}_{0.02}\text{K}_{0.01}\text{FePO}_4/\text{C}$ -TNAs and Electrochemical cycling at various C rates for d) TNAs, e) $\text{LiNa}_{0.02}\text{K}_{0.01}\text{FePO}_4/\text{C}$ and f) $\text{LiNa}_{0.02}\text{K}_{0.01}\text{FePO}_4/\text{C}$ -TNAs.

seen in other samples. It can also be seen from Fig. 4f that the $\text{LiNa}_{0.02}\text{K}_{0.01}\text{FePO}_4/\text{C}$ -TNAs full-cell displayed ~ 175 , ~ 127 , ~ 96 , ~ 69 , and $\sim 39 \text{ mAhg}^{-1}$ for 0.1, 0.5, 1, 2 and 5C rates, respectively. The rate capacity of the full cell is lower than both anode and cathode half-cells due to the lower ionic and electronic conductivity of both anode and cathode

in comparison to Li metal used in half-cells. It is worth mentioning that long-term cycleability studies are equally important as rate capability studies. Therefore, such studies were carried out at 0.5C rate and the data is shown in Fig. 5 as normalized reversible capacity vs. cycle number. The initial discharge capacity of 127.3 mAhg^{-1} is assumed as

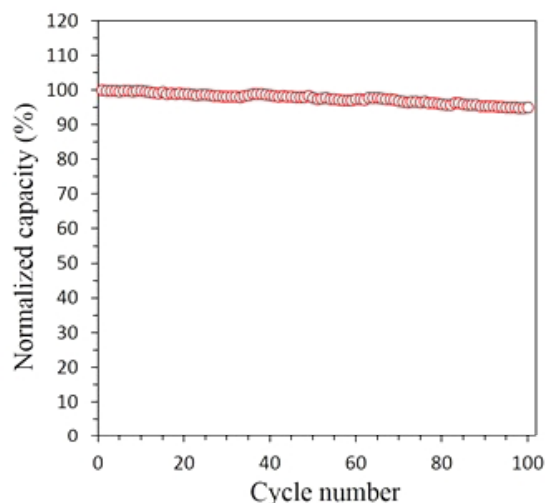


Fig. 5. Plot of normalized discharge capacity vs. cycle number for $\text{LiNa}_{0.02}\text{K}_{0.01}\text{FePO}_4/\text{C}$ -TNAs full-cell at 0.5C rate.

100%. Impressive and stable cycling profiles are observed for 100 cycles with capacity retention of ~95%. Therefore, the good rate capability and cycleability of the $\text{LiNa}_{0.02}\text{K}_{0.01}\text{FePO}_4/\text{C}$ -TNAs full-cell make it highly promising for practical application.

4. Conclusion

Firstly, TNAs and $\text{LiNa}_{0.02}\text{K}_{0.01}\text{FePO}_4/\text{C}$ composite were characterized in a half-cell configuration and subsequently were employed as a $\text{LiNa}_{0.02}\text{K}_{0.01}\text{FePO}_4/\text{C}$ -TNAs configuration in full-cell. In the full-cell, the $\text{LiNa}_{0.02}\text{K}_{0.01}\text{FePO}_4/\text{C}$ -TNAs assembly shows remarkable ~95% retention of the initial discharge capacity after 100 cycles at 0.5C rate, with an operating potential of ~ 1.7 V. The $\text{LiNa}_{0.02}\text{K}_{0.01}\text{FePO}_4/\text{C}$ -TNAs configuration with its excellent cycling and good rate performance is certainly useful for development of Li-ion battery for the stationary energy storage and in particular for community storage applications like EV and HEV.

Acknowledgement

We gratefully acknowledge financial support from the Research Council of Malek-Ashtar University of Technology.

References

- [1] Chen W. M., Qie L., Yuan L. X., Xia S. A., Hu X. L., Zhang W. X., Huang Y. H., "Insight into the improvement of rate capability and cyclability in $\text{LiFePO}_4/\text{polyaniline}$ composite cathode", *Electrochim. Acta*, 2011, 56: 2689.
- [2] Hassoun J., Pfanzelt M., Kubiak P., Wohlfahrt-Mehrens M., Scrosati B., "An advanced configuration $\text{TiO}_2/\text{LiFePO}_4$ polymer lithium ion battery", *J. Power Sources*, 2012, 217: 459.
- [3] Reale P., Fericola A., Scrosati B., "Compatibility of the Py24TFSI–LiTFSI ionic liquid solution with $\text{Li}_4\text{Ti}_5\text{O}_{12}$ and LiFePO_4 lithium ion battery electrodes", *J. Power Sources*, 2009, 194: 182.
- [4] Liu Y., Gorgutsa S., Santato C., Skorobogatiy M., "Flexible, Solid Electrolyte-Based Lithium Battery Composed of LiFePO_4 Cathode and $\text{Li}_4\text{Ti}_5\text{O}_{12}$ Anode for Applications in Smart Textiles", *J. Electrochem. Soc.*, 2012, 159: A349.
- [5] Brutti S., Hassoun J., Scrosati B., Lin C. Y., Wu H., Hsieh H. W., "A high power Sn–C/C– LiFePO_4 lithium ion battery", *J. Power Sources*, 2012, 217: 72.
- [6] Hassoun J., Lee D. J., Sun Y. K., Scrosati B., "A lithium ion battery using nanostructured Sn–C anode, LiFePO_4 cathode and polyethylene oxide-based electrolyte", *Solid State Ionics*, 2011, 202: 36.
- [7] Choi D., Wang D., Viswanathan V. V., Bae I. T., Wang W., Nie Z., Zhang J. G., Graff G. L., Liu J., Yang Z., Duong T., "Li-ion batteries from LiFePO_4 cathode and anatase/graphene composite anode for stationary energy storage", *Electrochem. Commun.*, 2010, 12: 378.
- [8] Rui X. H., Jin Y., Feng X. Y., Zhang L. C., Chen C. H., "A comparative study on the low-temperature performance of LiFePO_4/C and $\text{Li}_3\text{V}_2(\text{PO}_4)_3/\text{C}$ cathodes for lithium-ion batteries", *J. Power Sources*, 2011, 196: 2109.

- [9] Wang H. E., Jin J., Cai Y., Xu J. M., Chen D. S., Zheng X. F., Deng Z., Li Y., Bello I., Su B. L., "Facile and fast synthesis of porous TiO₂ spheres for use in lithium ion batteries", *J. Colloid Interface Sci.*, 2014, 417: 144.
- [10] Pan D., Huang H., Wang X., Wang L., Liao H., Li Z., Wu M., "C-axis preferentially oriented and fully activated TiO₂ nanotube arrays for lithium ion batteries and supercapacitors", *J. Mater. Chem. A*, 2014, 2: 11454.
- [11] Chiu K. F., Lin K. M., Leu H. J., Chen C. L., Lin C. C., "Fabrication and Characterization of Nano-Crystalline TiO₂ Thin Film Electrodes for Lithium Ion Batteries", *J. Electrochem. Soc.*, 2012, 159: A264.
- [12] He B. L., Dong B., Li H. L., "Preparation and electrochemical properties of Ag-modified TiO₂ nanotube anode material for lithium-ion battery", *Electrochem. Commun.*, 2007, 9: 425.
- [13] Zhang X., Aravindan V., Kumar P. S., Liu H., Sundaramurthy J., Ramakrishna S., Madhavi S., "Synthesis of TiO₂ hollow nanofibers by co-axial electrospinning and its superior lithium storage capability in full-cell assembly with olivine phosphate", *Nanoscale*, 2013, 5: 5973.
- [14] Zhang J., Zhang J., Ren H., Yu L., Wu Z., Zhang Z., "High rate capability and long cycle stability of TiO₂- δ -La composite nanotubes as anode material for lithium ion batteries", *J. Alloys Compd.*, 2014, 609: 178.
- [15] Qin G., Zhang H., Wang C., "Ultrasmall TiO₂ nanoparticles embedded in nitrogen doped porous graphene for high rate and long life lithium ion batteries", *J. Power Sources*, 2014, 272: 491.
- [16] Xue L., Wei Z., Li R., Liu J., Huang T., Yu A., "Design and synthesis of Cu₆Sn₅-coated TiO₂ nanotube arrays as anode material for lithium ion batteries", *J. Mater. Chem.*, 2011, 21: 3216.
- [17] Roy P., Berger S., Schmuki P., "TiO₂ Nanotubes: Synthesis and Applications", *Angew. Chem. Int. Ed.*, 2011, 50: 2904.
- [18] Djenizian T., Hanzu I., Knauth P., "Nanostructured negative electrodes based on titania for Li-ion microbatteries", *J. Mater. Chem.*, 2011, 21: 9925.
- [19] Su X., Wu Q., Zhan X., Wu J., Wei S., Guo Z., "Advanced titania nanostructures and composites for lithium ion battery", *J. Mater. Sci.*, 2012, 47: 2519.
- [20] Suresh Kumar P., Aravindan V., Sundaramurthy J., Thavasi V., Mhaisalkar S. G., Ramakrishna S., Madhavi S., "High performance lithium-ion cells using one dimensional electrospun TiO₂ nanofibers with spinel cathode", *RSC Adv.*, 2012, 2: 7983.
- [21] Aravindan V., Sundaramurthy J., Kumar P. S., Shubha N., Ling W. C., Ramakrishna S., Madhavi S., "A novel strategy to construct high performance lithium-ion cells using one dimensional electrospun nanofibers, electrodes and separators", *Nanoscale*, 2013, 5: 10636.
- [22] Game O., Kumari T., Singh U., Aravindan V., Madhavi S., Ogale S. B., "(0 0 1) faceted mesoporous anatase TiO₂ microcubes as superior insertion anode in practical Li-ion configuration with LiMn₂O₄", *Energy Storage Mater.*, 2016, 3: 106.
- [23] Armstrong G., Armstrong A. R., Bruce P. G., Reale P., Scrosati B., "TiO₂(B) Nanowires as an Improved Anode Material for Lithium-Ion Batteries Containing LiFePO₄ or LiNi_{0.5}Mn_{1.5}O₄ Cathodes and a Polymer Electrolyte", *Adv. Mater.*, 2006, 18: 2597.
- [24] Prosini P. P., Cento C., Pozio A., "Lithium-ion batteries based on titanium oxide nanotubes and LiFePO₄", *J. Solid State Electrochem.*, 2014, 18: 795.
- [25] Madram A. R., Daneshlab R., Sovizi M. R., "Effect of Na⁺ and K⁺ co-doping on the structure and electrochemical behaviors of LiFePO₄/C cathode material for lithium-ion batteries", *RSC Adv.*, 2016, 6: 101477.
- [26] Lee S., Park I. J., Kim D. H., Seong W. M., Kim

D. W., Han G. S., Kim J. Y., Jung H. S., Hong K. S.,
“Crystallographically preferred oriented TiO₂ nanotube
arrays for efficient photovoltaic energy conversion”,
Energy & Environ. Sci., 2012, 5: 7989.

[27] Shu Z. X., McMillan R. S., Murray J. J.,
“Electrochemical Intercalation of Lithium into Graphite”,
J. Electrochem. Soc., 1993, 140: 922.